Remote Sensing of Environment 210 (2018) 259–268

Contents lists available at ScienceDirect

Remote Sensing of Environment

journal homepage: www.elsevier.com/locate/rse

Land cover and land use change analysis using multi-spatial resolution data and object-based image analysis

Sory I. Toure[a,*], Douglas A. Stow[a], Hsiao-chien Shih[a], John Weeks[a], David Lopez-Carr[b]

[a] Department of Geography, San Diego State University, San Diego, CA 92182-4493, USA
[b] Department of Geography, 1832 Ellison Hall, University of California Santa Barbara, Santa Barbara, CA 93106-4060, United States

ARTICLE INFO

Keywords:
GEOBICA
Backdating
Urban
Land cover
Land use
Fine spatial resolution
Landsat
Change detection

ABSTRACT

Remote sensing data and techniques are reliable tools for monitoring and studying urban land cover and land use (LCLU) change. Fine spatial resolution (FRes) commercial satellite image in conjunction with geographic object-based image change analysis (GEOBICA) methods have been used to generate detailed and accurate urban LCLU maps. The integration of a backdating approach improves LCLU change classification results for the first date of a bi-temporal image sequences. Conversely, moderate spatial resolution satellite images such as those from Landsat sensors may not allow for detailed urban land use and land cover mapping. The objective of this study is to test a new bi-temporal change identification approach that integrates image classification of fine spatial resolution satellite imagery at time-2 and moderate spatial resolution satellite imagery (Landsat) at time-1, in a backdating and GEOBICA framework for mapping urban land use change. We compare the results from this approach to those of a GEOBICA approach based on fine spatial resolution imagery in both periods. The overall accuracy of the time-1 Landsat image classification is 0.82 and that of the fine spatial resolution image is 0.87. Moreover, the overall accuracy of the areal change data estimated from the pixel-wise spatial overlay of bi-temporal FRes LCLU maps is 0.80 while that from overlaying a time-2 FRes-generated map to that from a Landsat time-1 image is 0.81. The proposed method can be used in areas that lack FRes data due to limited coverage in the early 2000s.

1. Introduction

The exponential growth of the human population within the last two hundred years has caused important changes in the natural and built environments. The majority of the world's population now lives in urban centers, a shift from the past when people primarily lived in rural areas. Urban centers not only modify the natural environment that they are replacing, they also affect the well-being of the population living within them. Monitoring urban land cover and land use change is therefore important.

Remote sensing data of varying spatial resolutions and image change analysis techniques have been used to monitor changes in the urban environment. The spatial resolution of the dataset used in urban land cover and land use change (LCLUC) studies influences the level of detail of classification schemes and the accuracy of resulting maps. Momeni et al. (2016) compared the influence of spatial resolution, spectral band set and classification approach for mapping detailed urban land cover in Nottingham, UK, and found the spatial resolution to clearly be “the most influential factor when mapping complex urban environments.” They concluded that image classifications with Landsat and similar moderate spatial resolution satellite systems were often limited to a general urban class, while very fine spatial resolution (VHR) imagery allowed for the discrimination of many urban land use sub-types. Other urban studies confirm their analysis. For example, Wang et al. (2012) used Landsat TM/ETM+ data to map the urban expansion in China between 1990 and 2010. Urban areas, bare soil, bodies of water, and vegetation were their main mapping categories. Odindi et al. (2012) used Landsat 5 TM data to monitor major land cover and land use changes in Port Elizabeth, South Africa between 1990 and 2000. They applied a post-classification comparison approach to change identification approach (Jensen, 2016) to monitor the built up, bare surface, green vegetation, beach or dune, and water classes. On the other hand, Ma et al. (2015) mapped eight land cover and land use classes based on Chinese advanced fine-spatial resolution satellite imagery and an object-oriented approach. Their classification scheme included the residential, commercial/Industrial, and transportation classes. Bouziani et al. (2010) developed an automated multispectral segmentation algorithm by integrating existing digital maps and

* Corresponding author.
E-mail address: stoure@sdsu.edu (S.I. Toure).

https://doi.org/10.1016/j.rse.2018.03.023
Received 22 January 2017; Received in revised form 11 March 2018; Accepted 17 March 2018

spectral data. They also mapped detailed urban land use/land cover classes based on fine spatial IKONOS and QuickBird imagery.

Change detection can be performed through pixel- and object-based approaches. Several studies have demonstrated the advantages associated with geographic object-based image change analysis (GEOBICA) (Stow, 2009) compared to traditional per-pixel based change detection (Myint et al., 2011; Zhou et al., 2008). Geographic object-based image analysis (GEOBIA) (Hay and Castilla, 2008) approaches to image classification allow for multi-scale image analysis, more types of image features to be exploited for classification, and a great reduction in the occurrence of small, spurious pixel changes (Chen et al., 2012). Stow (2009) detailed the two general types of GEOBICA approaches to land cover and land use change mapping: 1) post-classification comparison where two separate GEOBIA land cover and land use maps are generated and spatially cross-tabulated, and 2) a multi-temporal layer stack approach where images for more than one date are segmented and resultant objects are classified as either land cover and land use transition classes or as no change. Multi-temporal time series of land cover maps can be generated by updating (projecting forward in time) and backdating (projecting backward in time) (Linke et al., 2009). Xian et al. (2009) developed a method to update the 2001 national land cover dataset (NLCD) to 2006. The method consists in identifying areas of land cover change occurring after 2001 and updating only those areas. For the areas that did not change, the original NLCD 2001 product is unchanged. In the updating/backdating approach, an existing map (often called the base map) is used as a starting point upon which subsequent classifications and change analyses are conducted. This approach has been shown to be both efficient and accurate (Linke et al., 2009; Xian et al., 2009). Yu et al. (2016) integrated the concept of updating/backdating with a GEOBICA approach to analyze land cover and land use change for the city of Beijing between 2001 and 2009. They found that the integration of the updating/backdating method to GEOBICA produced greater overall classification accuracies compared to an integration between the updating/backdating approach to a pixel-based analysis. They also found that the GEOBICA backdating approach greatly increased efficiency by focusing only on locations with changes. Toure et al. (2016) also integrated the backdating approach with GEOBICA and called it an object-based temporal inversion approach to urban land use change analysis. They also found that this approach improved the accuracy of time-1 LCLU maps, as well as that of the land use change classification products generated from fine spatial resolution satellite data for both dates of a bi-temporal image pair.

Past GEOBICA studies have involved datasets with similar spatial resolutions in time 1 and 2. Both the Yu et al. (2016) and Toure et al. (2016) studies that incorporated the backdating approach with GEOBICA, were based on datasets with similar spatial resolutions. Similarity includes near-anniversary dates of image capture, similar spatial, spectral, and radiometric resolutions, and approximately the same extents of coverage. However, this is not always achievable. No studies reported in the literature have used bi-temporal satellite images having very different spatial resolutions with a GEOBICA approach to land cover and land use change analysis. One reason is the unavailability of newer generation fine spatial resolution satellite imagery for historical dates. For example, fine spatial resolution imagery such as QuickBird or IKONOS became commercially available only in the late 1990s and early 2000s. Therefore, it is not possible to use them in change analyses that involve a date prior to 1999. Moreover, tropical regions of the world are affected with persistent cloud cover throughout most of the year, which makes it difficult to capture cloud-free and fine quality satellite imagery. Finally, commercial satellite coverage is partially driven by market potential; developing countries such as Ghana, the country within which our study area is located, may not have been considered a high value market such that tasking and capturing imagery for such countries occurred less frequently at the start of the commercial satellite era (c.2000).

Updating (projecting forward in time) and backdating (projecting backward in time) require a very accurate base map that provides partial basis for generating the land cover and land use map representing the other point in time. For example, the National Land Cover Database (NLCD) 2001 base map used to create the NLCD 2006 through the updating process is based primarily on a decision-tree classification of c.2001 Landsat satellite data and is comprised of three elements: land cover, percent developed impervious surface and percent tree canopy density. It does not contain a detailed urban land use classification scheme. Obtaining land use classes more specific than developed impervious will require dataset that have finer spatial resolutions than Landsat, and such fine spatial resolution images are more available after 2000. Backdating would be more appropriate in change identification studies that have finer spatial resolution data for the later period.

The objective of this paper is to test the accuracy of performing land cover and land use change analysis with a fine spatial resolution imagery for the second period and moderate resolution (Landsat 7 ETM+) imagery for the first period using an integrated backdating and GEOBICA approach. Specifically, the research questions are:

1. What is the utility of a post-classification change identification approach that is based on an initial object-based classification of a fine spatial resolution time-2 image, which is used to constrain the segmentation and subsequent classification of a time-1 moderate spatial resolution image?; and
2. Given the classes of interest (residential, non-residential, and non-built) for our broader study of drivers and impacts of land cover and land use change in major urban areas of Ghana, how accurately can land use be mapped based on Landsat ETM+ moderate spatial resolution satellite imagery?

2. Methodology

2.1. Study area and data

The study area is located in the Greater Accra region in southern Ghana (Fig. 1). The 545-km^2 study area consists of the entire Accra Metropolitan Area (AMA) and parts of seven other census districts: GA West, Ga East, Ga South, Ledzokuku/KROWOR, Adenta, Tema, and Ashaiman. Accra, the capital city of Ghana has experienced substantial population growth and built-up land since the country's independence in 1957. The population of Ghana grew from 5 million in 1950 to 25 million in 2010 (Ghana Statistical Services, 2012). Most of the population growth occurred in urban centers due to natural growth and internal migration. Only 15% of the population lived in urban areas in 1950 compared to 52% in 2010. The total urban area of Accra and its surrounding suburbs, regardless of the administrative boundaries, covered 216 km^2 in 1985, 276 km^2 in 1991, and 555 km^2 in 2002 (Møller-Jensen et al., 2005). The climate of the study area is tropical wet and dry and varies along an aridity gradient from the wetter coastal areas to drier parts inland. The prevalence of persistent cloud cover throughout the year as well as the harmattan, a dry, dust-laden wind in November–March, limits the availability of clear images. The equatorial vegetation that once covered the study area has been replaced by habitation, secondary forests, agricultural development and shrub thicket (Stow et al., 2016).

The study period for this research is the decade between 2000 and 2010. The period was selected as to coincide with the Ghanaian population and housing census, and to correspond with the availability of fine spatial resolution commercial satellite imagery for some portions of the study area.

Information about the data used in the study is listed in Table 1. Five and eight fine spatial resolution commercial satellite images were selected for the time period c.2000 and c.2010 respectively. These image data were made available to us at no cost through a NASA and National Geospatial Intelligence Agency (NGA) agreement. It was

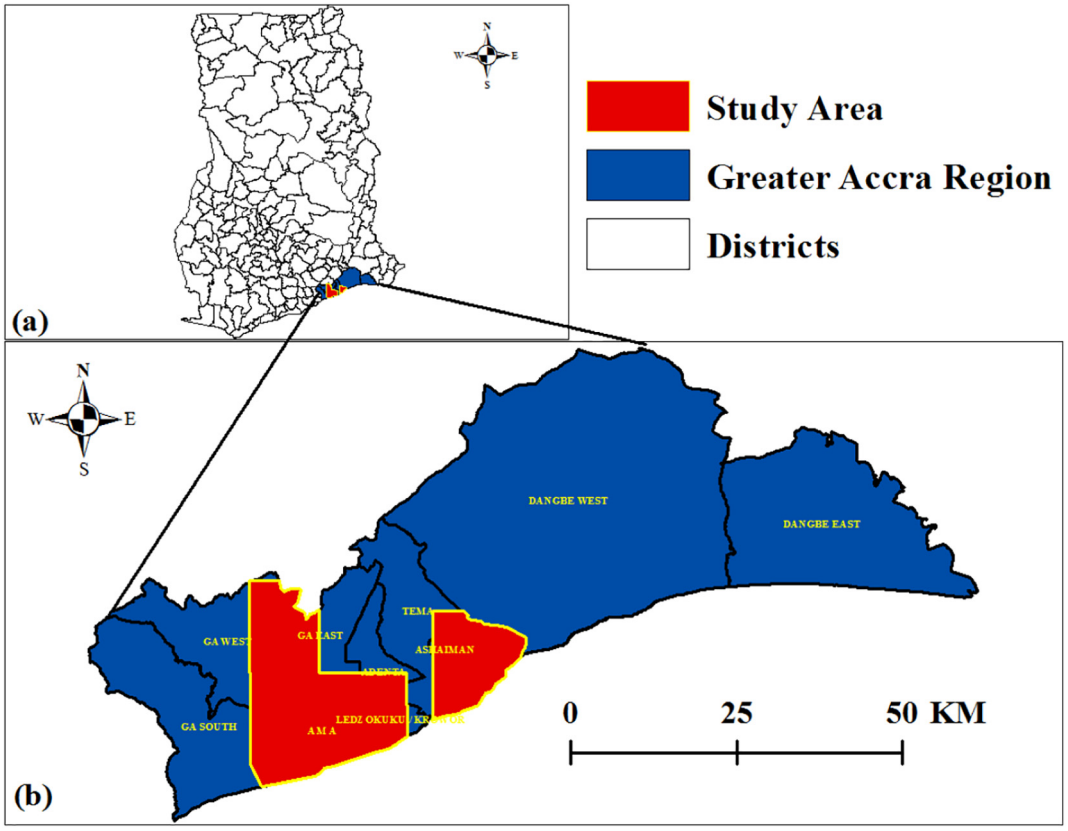

Fig. 1. Study area. (a) Greater Accra region within Ghana; (b) study area within the greater Accra region. Polygons represent districts.

Table 1
List of image data set used in the study.

Satellite sensor	Temporal coverage	Spectral bands	Spatial resolution
Landsat ETM+	2002	VNIR, SWIR	30 m MS, 15 m PAN
IKONOS	2000 February 10	VNIR	3.2 m MS, 0.8 m PAN
QuickBird-2	2002 April 12	VNIR	2.4 m MS, 0.6 m PAN
IKONOS	2002 May 22	VNIR	3.2 m MS, 0.8 m PAN
QuickBird-2	2003 December 18	VNIR	2.4 m MS, 0.6 m PAN
IKONOS	2004 April 10	VNIR	3.2 m MS, 0.8 m PAN
QuickBird-2	2009 April 15	VNIR	2.4 m MS, 0.6 m PAN
WorldView-02	2010 January 12	VNIR	1.8 m MS, 0.46 m PAN
QuickBird-2	2010 January 13	VNIR	2.4 m MS, 0.6 m PAN
GeoEye-1	2010 February 15	VNIR	1.65 m MS, 0.4 m PAN
WorldView-02	2010 March 27	VNIR	1.8 m MS, 0.46 m PAN
GeoEye-1	2010 April 13 (3 images)	VNIR	1.65 MS, 0.4 m PAN

necessary to use several images for both dates to cover the entire study area and to substitute or composite areas having cloud cover. The c.2000 images cover the period 2000–2004 while seven of the time-2 (c.2010) images were taken in 2010 and one in 2009. These included multispectral image data from IKONOS, QuickBird, WorldView-02, and GeoEye satellite imaging systems, with spatial resolutions varying between 1.65 m and 3.4 m. All images have a panchromatic band and at least three visible (V) and one near infrared (NIR) multispectral bands, except the WorldView-02 images which have eight multispectral bands. A Landsat 7 ETM+ satellite image acquired on December 26, 2002 was used for the time-1 period; this is the only completely cloud-free ETM+ image covering the study area captured between 1999 and 2013. ETM+ images have a nominal spatial resolution of 30 m and can be obtained in an orthorectified format at Level 1 T from the Land Processed Data Active Archive Center. ETM+ images have seven multispectral bands and one panchromatic band of 15 m. The ETM+ thermal infrared band (6) was not utilized.

The fine spatial resolution satellite images were orthorectified to provide accurate spatial positioning between the multitemporal images. Horizontal ground control points (GCPs) were selected from DigitalGlobe images available in Google Earth. Elevations for GCPs were extracted from NEXTMap World 30, a digital elevation data purchased from Intermap. The GCPs were then incorporated into the orthorectification process, with bi-linear interpolation algorithm and a second-order polynomial refinement of image registration.

We are interested in knowing the major urban landscape features, and how the physical environment is affected by urban development. Therefore, the major land use types in our classification scheme include residential built (residential for short), non-residential built (non-residential for short), and non-built categories, while the land cover classes that compose land use units are vegetation, impervious and soil. The residential class includes high and low socio-economic status neighborhoods, or other places where people primarily reside. Industries, institutions such as school and office buildings, commercial areas and ports are all included in the non-residential class. The non-built class includes places such as agricultural plots, or undeveloped areas.

Vector GIS data representing the streets of Accra were downloaded from the Open Street Map (OSM) website and used as auxiliary data. Street data were used in the segmentation phase to generate regularly shaped land use objects. Their attributes were also used as additional feature inputs to aid in classifying land use classes. OSMs are user-generated street maps that follow the peer production model created by Wikipedia (Haklay and Weber, 2008). Contributors to the OSM project use areal imagery, GPS devices, and other tools in order to ensure the accuracy of OSM maps (http://www.openstreetmap.org/about).

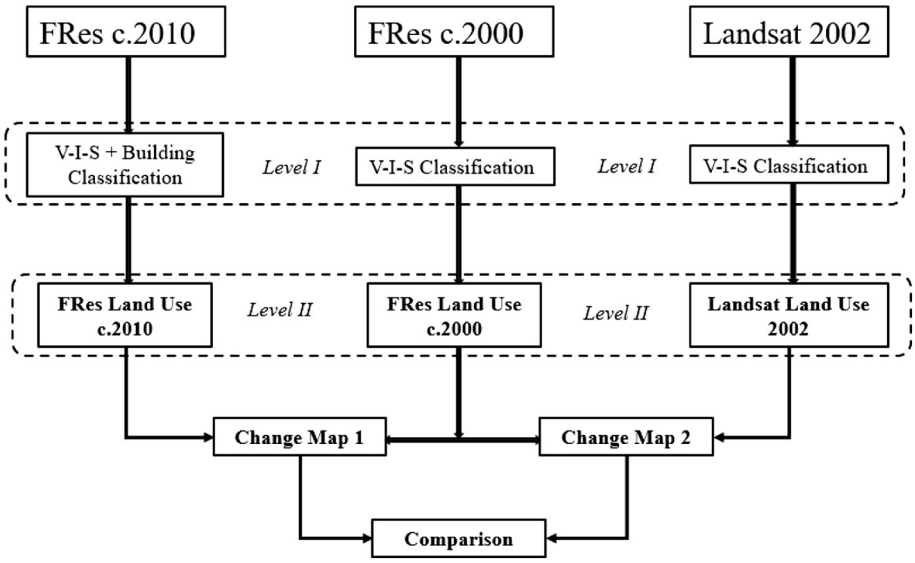

Fig. 2. General classification strategy. V-I-S: Vegetation, impervious, soil. FRes: fine resolution.

2.2. Image processing

The general image classification and change estimation processing flow for the study is shown in Fig. 2. It consists of generating two different land use change maps and comparing their results. One land use change map was generated by comparing fine spatial resolution imagery in time-1 and time-2. The other was produced by comparing fine spatial resolution images in time-2 to a moderate spatial resolution Landsat image in time-1. We adopted an OBIA approach using eCognition software to segment and classify all the images. The time-2 images were first classified and the classification results were incorporated into the time-1 classification procedures using the backdating approach. The following sections describe in detail the classification procedures for each image in their respective order.

2.2.1. c.2010 FRes land use classification

Eight multispectral images from c.2010 were classified individually using the same procedures, and the resultant land use (LU) maps were mosaicked to create a single time-2 (c.2010) product. Four steps constituted the general workflow: 1) Vegetation-Impervious-Soil (VIS) classification, 2) buildings classification, 3) integration of the buildings and the VIS classification products, and 4) land use classification. The VIS classification was necessary to differentiate developed from non-built land uses. We classified buildings and their size to separate residential land use from non-residential land use. We found in a preliminary analysis of the study area that large buildings were characteristics of the non-residential land use type. We adopted and modified the classification strategy of Toure et al. (2016). The procedures followed the three general steps of OBIA, which are segmentation, classification, and generalization. Two maps of differing scale hierarchy were generated for all multispectral images, a finer-scale (Level I) map and a coarser-scale (Level II) land use map. The target classes in Level I were vegetation, impervious, and soil classes. A building class was also added to the Level I classification for the c.2010 images. The target land use classes in Level II were residential, non-residential, and non-built. The Level I objects were sub-objects of the Level II land use objects.

We first created the Level II segments with the multiresolution segmentation algorithm. The segmentation was constrained by using the OSM roads layer as auxiliary data, such that the resulting land use objects corresponded to city blocks naturally occurring in the city. The specific scale parameters were different from image to image because they have different spatial resolutions. However, we included all the multispectral bands of each image during the segmentation phase, and kept the compactness and shape index values constant at 0.5 and 0.5 respectively. The VIS segments were then created as sub-objects to the land use segments with the multiresolution segmentation algorithm.

After the segmentation stage, Level I image objects were classified as either vegetation, impervious, or soil. The vegetation class was separated from other non-vegetation categories by using the normalized difference vegetation index (NDVI). NDVI thresholds were chosen interactively and were different for each image. The remaining image objects were classified as either impervious or soil. It was sometimes necessary to create two spectral sub-classes, (dark and light) for impervious and soil classes because they appear different throughout the study area. Brightness, red, green, blue, NDVI, NDWI, and the Red/Green normalized difference index were the features used to define and separate the four subclasses. Normalized Difference Water Index (NDWI) is calculated as (Green − NIR)/(Green + NIR) (McFeeters, 1996) while the Red/Green normalized difference index is calculated as (Red Edge − Green)/(Red Edge + Green), (Belgiu et al., 2014). Object classification was based on the combination of the mean feature values of each segment. We classified the remaining image objects after the class definition phase.

Buildings were classified separately to increase efficiency and computational speed. We used the fused panchromatic and multispectral (i.e., pan-sharpened) images for the classification. A pan-sharpened image was created for each fine spatial resolution image using the multiple routines in ERDAS Imagine software. The WorldView-02 images were pan-sharpened using the Hyperspherical Color Space (HCS) Resolution Merge algorithm. We used the Subtractive Resolution Merge algorithm to pan-sharpen the QuickBird, Ikonos, and GeoEye-1 images. The strategy with the building classification phase was to first mask out non-building elements, and then focus on the buildings. NDVI was used to classify the vegetation class. We classified the roads by first segmenting the images with the multiresolution segmentation algorithm and using the OSM vector layer as a thematic layer. The segmentation scale parameter was kept below 25 for the different images while the shape and compactness criteria were 0.5 and 0.5 respectively. Image objects that touched roads from the road layer were assigned to the road class. The green spectral band was used to differentiate shadow from non-shadow elements. Segments with relatively small mean green values were classified as shadow in certain images. The remaining unclassified image-objects were merged. The bright and dark edges in the unclassified area were enhanced using edge extraction algorithms. The edge enhanced image was then

segmented and classified into edges inside bright objects and edges outside bright objects. Non-building edges were removed by applying the following conditions. Any bright edge objects that were beyond a threshold distance from any dark edge objects were unclassified, while any dark edge objects beyond the threshold from any bright edge objects were also unclassified. Building objects were constituted as any unclassified areas that were completely enclosed by an edge object. The objects classified as buildings were merged and exported as thematic raster data.

The building objects file was integrated as a thematic layer with the VIS classification product, such that the VIS level (Level I), a level with image objects that are sub-objects to the land use (Level II) objects, had four classes for the c.2010 classification: vegetation, impervious, soil, and buildings. We then implemented a rule stating that any image object classified as impervious and spatially corresponding to a building is assigned to the building class.

Level II segments were classified as a residential, non-residential, or non-built land use category through a series of rules with the vegetation-impervious-soil and building classification as input. The presence/absence or abundance of edges in the image was also an important factor in discriminating between the different land use types. We used the Sobel filter (Gupta and Mazumdar, 2013), an edge-detection algorithm, to enhance edges in the image. We created a new image layer called *SobelRed* by applying the *Sobel Edge Filter* algorithm to the red band with a window size of 3×3 to the unclassified image objects. Segments having $\geq 90\%$ vegetation and soil areal cover were classified as non-built. Segments having small mean *SobelRed* values, an indication of the presence of few built-up structures, were also classified as non-built. A Level II image object with a relatively large mean building size was classified as non-residential. The sizes of buildings were determined through preliminary analysis to be an important indicator of non-residential areas. Moreover, image texture was also a good discriminator of the non-residential land use. We adopted a statistical method of examining texture that considers the spatial relationship of pixels called the gray-level co-occurrence matrix (GLCM). Larger values of the GLCM homogeneity feature indicated non-residential areas. Finally, the remaining Level II segments were classified as residential. The resultant classification product was exported as a vector layer and used as a thematic input to the classification of the c.2000 fine spatial resolution and moderate spatial resolution images.

2.2.2. c.2000 FRes land use classification and change identification

The fine spatial resolution images dating from c.2000 were classified individually and then mosaicked to create a single c.2000 land use product. We followed the same land cover and land use classification steps described above for the c.2010 images, but integrated the c.2010 classification results through the backdating approach. We first created Level II land use image-objects by applying the multiresolution segmentation algorithm. However, we used the c.2010 classification result as thematic layer such that the c.2000 segments either followed the c.2010 image objects boundaries or were completely contained within them. We maintained the shape and compactness criterion at 0.5 and 0.5 respectively for all images. We chose scale parameters that would create image objects with sizes as large as the c.2010 image objects or smaller; these parameter values varied between 50 and 200. Once the Level II image objects were created, we created Level I VIS sub-objects in a similar manner as for the time-2 images. We then classified Level I image objects as vegetation, impervious, soil, with the methods described above.

The land use classification of the c.2000 Level II image objects was achieved through backdating. We first located areas of no change. Undeveloped areas in 2010 were almost certainly non-built in 2000. We therefore assigned to the non-built class any c.2000 areas that were classified as non-built in the c.2010 map. We then classified other non-built areas in the c.2000 images through the series of rules described above for c.2010. The remaining areas were classified as residential or non-residential through the backdating approach. Areas classified as residential and non-residential in the c.2010 map were assigned to the residential and non-residential classes respectively in 2000.

We estimated areas that developed to urban (residential or non-residential) between 2000 and 2010. Any areas classified as non-built in 2000 and residential in 2010 were assigned to the *to Residential* class while non-built areas classified as *non-residential* in 2010 were classified as *to Non-Residential*.

2.2.3. c.2000 Landsat land use classification and change identification

The land use classification of the moderate spatial resolution Landsat image was conducted in a similar manner to that of the c.2000 fine resolution images. We first created level II land use objects by applying the multiresolution segmentation algorithm with the c.2010 map as thematic layer. The shape and compactness criterion selected interactively were both 5. A scale parameter of 100 was selected, which is smaller than that of the fine spatial resolution images because of the difference in spatial resolutions. We then created level I VIS objects as sub-objects to the level II with the multiresolution segmentation routine. We classified these Level I segments as vegetation, impervious, and soil. NDVI was used to classify the vegetation as with the fine spatial resolution imagery, while the input features used to classify the soil and impervious classes were different in the case of the Landsat image. The green and SWIR1 spectral bands, combined with the fuzzy operator AND, were used as classification feature inputs.

The land use classification and change identification procedures for mixed spatial resolution images were similar to that of the c.2000 FRes data. Areas classified as non-built in 2010 were considered non-built in 2000. Places having 90% or more of vegetation and soil or areas with small mean *SobelRed* value were also classified as non-built. The remaining developed areas were classified as either residential or non-residential following their classification in 2010 through the backdating approach. Places classified as non-built in 2000 and classified as residential and non-residential in 2010 were assigned to the *to residential* and *to non-residential* classes respectively in the change map.

2.3. Accuracy assessment

We performed an accuracy assessment on the land use classification products from Landsat (time-1) and the fine spatial resolution satellite (time-1 and 2) image sets, as well as the two land use change (LUC) maps generated from different time-1 maps. We designed the accuracy assessment with the objectives of estimating overall and class-specific accuracies, areas of the individual classes (as estimated by the reference classification), and confidence intervals for each accuracy and area parameter. The spatial unit of assessment was a square polygon of size 100 m × 100 m.

We implemented procedures in Olofsson et al. (2014) for the accuracy assessment in this study. We adopted a stratified random sampling design with the classes of the maps as strata because it satisfies the accuracy assessment and area estimation objectives. We used the equation provided by Cochran (1977, Eq. (5.25)) to determine the samples sizes (n):

$$n = \left(\frac{\sum W_i S_i}{S(\widehat{O})} \right)^2 \quad (1)$$

where W_i is the proportion area for each class i, and S_i is the standard deviation of the user's accuracy of stratum i, and $S(\widehat{O})$ is the standard error of the estimated overall accuracy that we sought to achieve. From Eq. (1), we selected a sample size of about 1000 (n = 998). We allocated 100 sample units to each of the change classes. The number of sample units for the remaining classes was determined by multiplying their respective areas by a constant selected interactively. Table 2 shows the distribution of sample units per class and map type.

The reference data used for the accuracy assessment were generated

Table 2
Sample size distributions of accuracy assessment units per class and map type. FRes = fine resolution. n = 998.

	c.2010 FRes.	c.2000 Fres.	Landsat 2002	FRes to FRes change map	FRes to Landsat change map
1. Residential	485	385	385	385	385
2. Non-residential	210	110	110	110	110
3. Non-built	303	503	503	303	303
4. Non-built to residential				100	100
5. Non-built to non-residential				100	100

by visual interpretation of the original fine spatial resolution images, along with Google Earth historical images acquired around the time-1 date, by an independent interpreter who is familiar with land use types of the study area. The good practice recommendations of Olofsson et al. (2014) states that if the same data are used to generate both the map and reference classifications, the process of creating the reference data should be of a higher quality than a satellite-based land cover and land use map, in terms of accuracy and reliability. The sample units were visually interpreted and land use class recorded by a well-trained analyst not familiar with the map products. We assumed that visual interpretation and manual classification would produce better base maps than the maps produced through supervised classification by integrating the GEOBICA and backdating approach. Despite the greater degree of confidence in the reliability and accuracy of the base maps, they certainly contain errors due to differences in classification rules, partial membership of more than one class per sampling unit, and uncertainty associated with co-location of sample units. The reference sample units were overlain on the different classification products to extract the majority class for that unit.

We generated accuracy/error matrices for each land use classification and land use change product. We report the error matrix in terms of estimated area proportion. The cell entries of the error matrix are estimated using equation:

$$\hat{p}_{ij} = W_i \frac{n_{ij}}{n_{i.}} \quad (2)$$

where W_i is the proportion of area mapped as class i, n_{ij} is the sample count at the particular cell, and n_i is the number of selected sample units for class i. Overall accuracy, producer's accuracy, user's accuracy, class area, as well as confidence intervals were estimated for each error matrix. The 95% confidence level for each class (i.e. the five types of land use change) is reported in order to quantify sampling variability of the accuracy and area estimates. We also include qualitative spatial overlay comparisons of the time-1 and land use change products to examine differences in the spatial representations of land use patterns between these products.

3. Results

3.1. Classification accuracy and spatial distributions of c.2010 land use

The estimated overall accuracy for the c.2010 land use classification product from fine spatial resolution image data is 0.89 ± with a 95% confidence interval of 0.018. The producer's accuracies for residential and non-built classes are 0.92 and 0.86 respectively. The non-residential class has the smallest producer's accuracy of 0.73 and the smallest user's accuracy of 0.48. The residential and non-built classes' user's accuracies are 0.89 and 0.96 respectively.

The area estimate with a 95% confidence interval of the residential class is 288.83 ± 9.82 km^2. The residential class covers the largest proportion of the study area and is mostly concentrated in the southern part of the study area within the AMA. The non-built class covers 229.14 ± 8.90 km^2 and is located in the northern and western part of the study area. Much of the area around the University of Ghana, Legon, the Accra International airport and between the AMA and Tema consists of non-built land use types. The area estimate of the non-residential built class with a 95% confidence interval is 27.06 ± 4.97 km^2. Commercial structures are concentrated along major freeways, especially the Accra-Tema motorway, the port in Tema, the airport, and in downtown Accra. Institutions such as schools are distributed fairly evenly throughout the study area.

3.2. Classification accuracy and spatial distributions of c.2000 land use

The estimated overall accuracy of the c.2000 fine spatial resolution (FRes) map is 0.87 while that of the Landsat is 0.82. The producer's accuracies of the residential and non-residential classes are larger for the time-1 FRes map compared to the map estimated with the Landsat back-dating approach. Their respective values are 0.91 and 0.64 in the former, and 0.86 and 0.38 in the latter. The residential and non-residential classes user's accuracies however are comparable in the Landsat-based map as compared to the FRes map; (0.86 vs. 0.83) for the residential class and (0.35 vs. 0.33, respectively) for the non-residential class. The non-built class user's and producer's accuracies are 0.96 and 0.86 respectively in the FRes map, and 0.85 and 0.85 in the Landsat 2002 map.

The area estimate with a 95% confidence interval of the residential class is 197.16 ± 9.64 km^2 and 242.71 ± 11.13 km^2 of the study area in 2000 for the FRes and Landsat map respectively. Undeveloped areas cover 332.98 ± 10.14 km^2 in the FRes map compared to 270.42 ± 11.97 km^2 in the Landsat map. The non-residential class covers less areal extent with 14.89 ± 4.30 km^2 and 31.90 ± 7.00 km^2 in the FRes and Landsat map respectively. However, differences exist in the spatial distribution of the classes. The residential and non-residential classes visually appear to be more fragmented in the FRes classification and more compact in the Landsat map. Moreover, the FRes map presents more non-built areas within the city boundaries as compared to the Landsat map. Some of these non-built areas are misclassifications of residential areas with a substantial amount of vegetation as non-built. Finally, spatial differences in the classification products exist in some areas (i.e., the same area is classified residential in one map and non-built in the other).

3.3. Classification accuracy and spatial distributions of 2000–2010 land use change

The land use change maps generated by post-classification comparison of the FRes time-1 and time-2 FRes maps and the Landsat time-1 and FRes time-2 maps are depicted in Figs. 3 and 4 respectively. The accuracy assessment results of both maps are presented in Tables 3 and 4 respectively. The overall accuracy of the FRes to FRes change map (change map 1) is 0.80 ± 0.023, and is 0.81 ± 0.021for the Landsat to FRes change map (change map 2). Changes from non-built to residential and non-residential have larger producer's accuracies in change map 1 compared to change map 2 at 0.53 > 0.42 and 0.39 > 0.24, respectively. The users' accuracies of the changed classes are also greater in change map 1 in comparison to change map 2: 0.57 vs. 0.42 for non-built to residential and 0.48 vs. 0.25 for non-built to non-residential.

About 19% (18.6%) of the study area changed between 2000 and 2010 according to Change map 1, corresponding to an area of 101.4 km^2 (Table 5). The changes from non-built to residential represent 85.00% (86.16 ± 11.63 km^2) of total change area, with non-built to non-residential constituting the remaining 15.00% (15.23 ± 4.54 km^2). Change map 2 depicts an overall change of

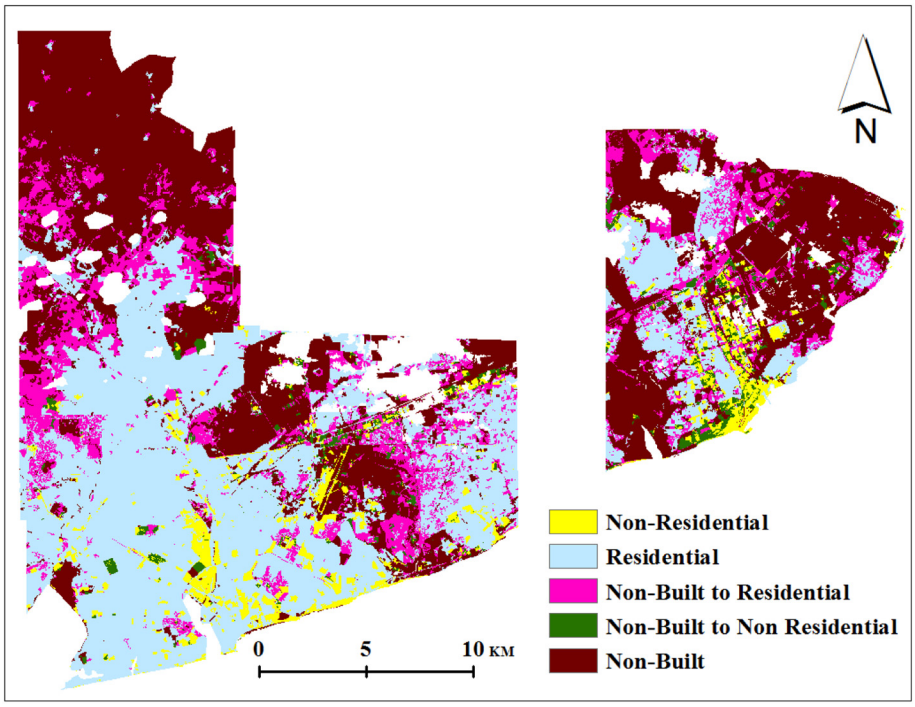

Fig. 3. FRes to FRes Land use change map.

11.74% (63.97 km^2) during the study period, 89% (56.78 ± 10.06 km^2) of which represents changes from non-built to residential and 11.00% (7.19 ± 3.39 km^2) from non-built to non-residential. Most of the residential expansion occurred at the city's edges in both maps. Change to non-residential areas occurred as infill within the city's boundaries in places that were adjacent to extant non-residential land use.

4. Discussion

The backdating approach played an important role in improving the overall classification results of the single date images. Change map 1 represented the greatest area of change (17%) in the Accra study area. Therefore, the overall accuracies of the time-1 images are highly dependent on the time-2 classification accuracy. The range of the overall classification accuracies for the two single-date land use classifications with fine spatial resolution, (i.e., time-2 FRes and time-1 FRes,) is only 0.02. The time-1 Landsat classification exhibits the smallest overall

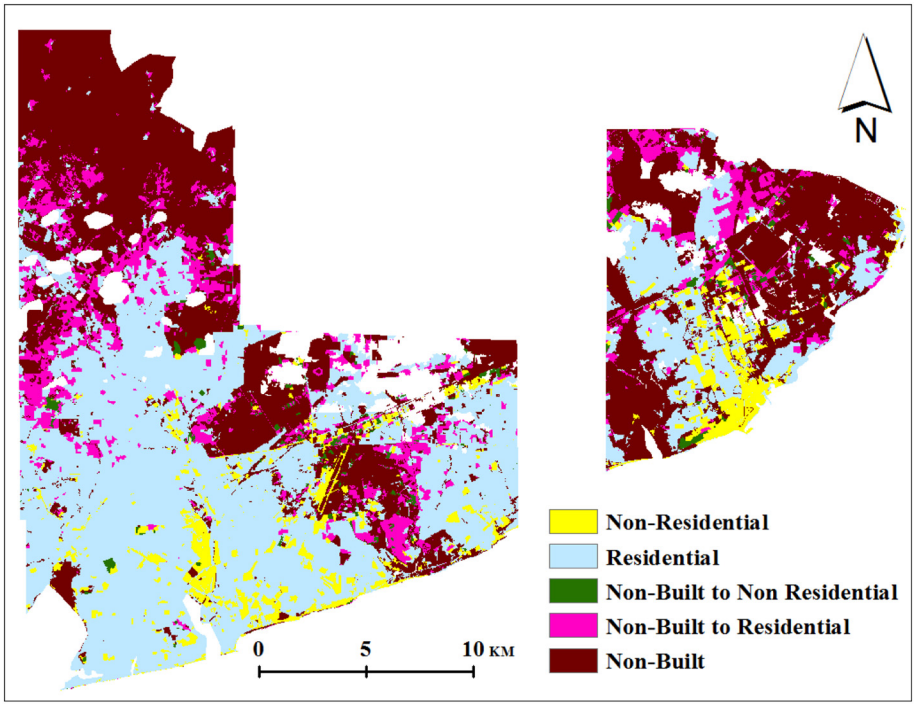

Fig. 4. FRes to Landsat Land use change map.

Table 3
c.2000 (FRes) to c.2010 (FRes) land use change identification accuracy assessment results.[1]

	Reference						
		Residential	Non-residential	Non-built	Non-built to residential	Non-built to non-residential	Total (W_i)	Area
Map	Residential	0.3301	0.0010	0.0135	0.0479	0.0083	0.4009	36,701,326
	Non-residential	0.0162	0.0171	0.0100	0.0048	0.0043	0.0523	4,786,353
	Non-built	0.0000	0.0000	0.3623	0.0149	0.0000	0.3773	34,536,731
	Non-built to residential	0.0176	0.0000	0.0411	0.0837	0.0044	0.1468	13,435,891
	Non-built to non-residential	0.0005	0.0018	0.0027	0.0068	0.0109	0.0228	2,085,989
	Total	0.3643	0.0200	0.4297	0.1581	0.0279	1.0000	91,546,291

[1] The cell entries are the products of the proportions and the stratum weights, as expressed in Eq. (2).

accuracy of 0.82. The difference in the overall accuracy of the two change maps is also only 0.01. The residential built and non-built classes were classified with large accuracies in the time-2 FRes dataset as well as in both of the time-1 datasets. On the other hand, the small classification accuracy of the non-residential built class in time-2 propagated in both time-1 classifications, as a result both image sets yielded smaller classification accuracies for this class.

We integrated the OSM vector data as auxiliary data to the segmentation of the time-2 images. The resulting segments represented the land use of interests. Constraining time-1 segmentation with segments from time-2 also created image-objects in time-1 that either followed the time-2 segments boundaries or were contained within them. Adopting such strategy reduces false changes due to misregistration between images in time-1 and 2. The GEOBICA approach also allowed us to implement our expert knowledge in combining the VIS and building classifications to generate the final land use classification. The ability to integrate one or more features in the classification phase potentially improves accuracies. The non-built class was mapped accurately across all image products, by combining the vegetation and/or the soil classifications. The *SobelRed* feature was also useful to map the non-built class in areas where these two land cover classes could not be separated.

The relatively simple classification scheme was certainly instrumental in achieving large overall accuracies of the single date classifications. The fact that we classified only three land use types, (residential, non-residential, and non-built) based on very fine spatial resolution imagery explains well why overall accuracies are above 80%. We did not map sub-classes within these general land use types, partly because of the desire to achieve sufficiently large map accuracies.

Several factors explain the resultant map accuracies of the individual land use classes. The residential class is apparently over-classified (more land area allotted to this class through image classification compared to the area estimated by the reference data), as indicated by the user's accuracies being smaller than the producer's accuracies. Mixed land uses are very prevalent in Accra. It is not uncommon to have both a residence and a business housed in the same building in many parts of the city. Our mapping strategy was to err on the side of inclusion. We therefore assumed the residential class to be the default land use for the entire city. Places that were not classified as either non-built or non-residential were assigned to the residential class. Confusion between the soil and impervious land cover classes led to the misclassification of several residential areas as non-built. The classification accuracies of the non-residential built class were the smallest of the three classes primarily because of the great variation in characteristics that define the sub-classes of this land use. Large building sizes and larger values of GLCM homogeneity were the primary features used to map this class. Misclassification of buildings was a source of error for the non-residential class. It was challenging to delineate single buildings and estimate their size in densely built parts of the city. Moreover, areas with larger GLCM homogeneity values tended to be non-residential. However, small density residential areas at the city's outskirts also tend to have larger GLCM homogeneity values, a cause of confusion between this class and the non-residential class.

Table 5
Land cover and land use change percentages.

	No change			Change	
	RB	NRB	NB	NB to RB	NB to NRB
2000 FRes to 2010 FRes map	36.43%	2.00%	42.97%	15.81%	2.79%
2002 Landsat to 2010 Fmap	43.41%	3.21%	41.63%	10.42%	1.32%

RB = residential built; NRB = non-residential built; NB = non-built.

Differences in the spatial extent and location of land use between the time-1 maps generated from the commercial satellite and Landsat image data are depicted in Fig. 5. Map differences are mainly due to differences in spatial resolutions of the dataset used in the study, and mostly occur in areas of active urban expansion where residential development occurred. Land use in these areas is classified as both residential and non-built in the FRes map, while they are completely classified as residential in the Landsat-estimated map. Non-residential areas tend to be composed of multiple land cover types. While large land use polygons were classified as non-residential built in the Landsat image, buildings were classified as non-residential built and the vegetation and soil as non-built in the FRes time-1 image. The moderate spatial resolution of the Landsat image generalizes or integrates land cover units within land use polygons. The result is that 5% more built areas (residential and non-residential) were mapped in the Landsat map than in the time-1 FRes map.

Table 4
c.2000 (Landsat/backdating) to c.2010 (FRes) land use change identification accuracy assessment results.

	Reference						
		Residential	Non-residential	Non-built	Non-built to residential	Non-built to non-residential	Total (Wi)	Area
Map	Residential	0.3812	0.0058	0.0127	0.0404	0.0046	0.4448	40,716,353
	Non-residential	0.0230	0.0224	0.0121	0.0035	0.0023	0.0633	5,792,641
	Non-built	0.0012	0.0000	0.3602	0.0149	0.0000	0.3763	34,450,873
	Non-built to residential	0.0268	0.0000	0.0299	0.0432	0.0031	0.1029	9,424,335
	Non-built to non-residential	0.0019	0.0039	0.0015	0.0022	0.0032	0.0127	1,162,090
	Total	0.4341	0.0321	0.4163	0.1042	0.0132	1.0000	91,546,291

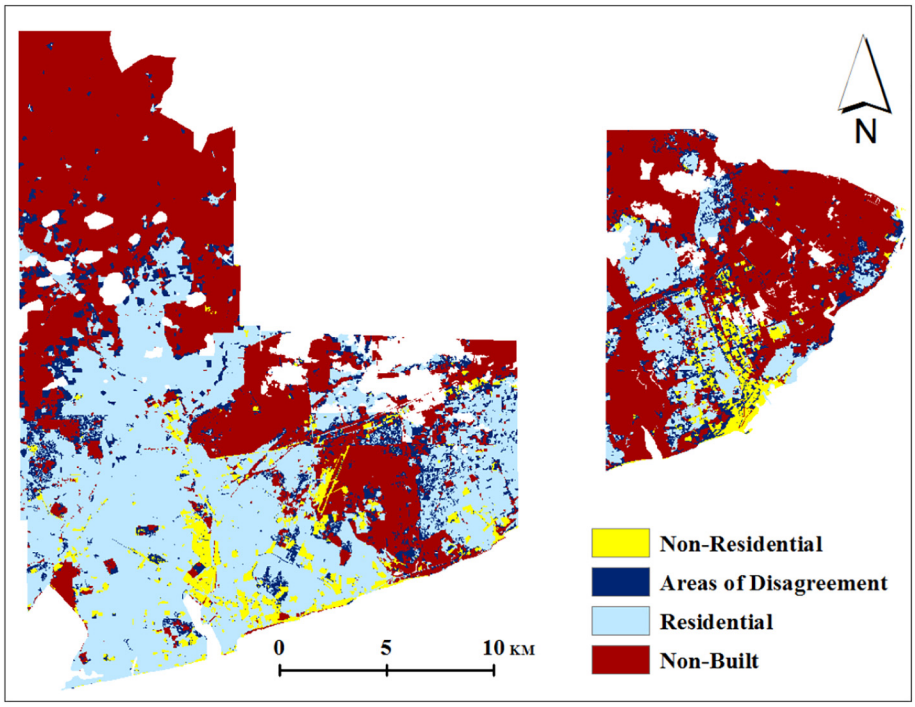

Fig. 5. Spatial overlay of the FRes and Landsat maps from c.2000.

5. Conclusions

Our study demonstrates the feasibility of performing relatively accurate urban land use and land cover change analysis based on datasets that have very different spatial resolutions. We evaluated a change detection method that compared a fine spatial resolution satellite image in time-2 to a Landsat image in time-1, due the lack of FRes satellite image coverage for the c.2000 period for much of our study area. We compared the land cover and land use change map from a backdating, GEOBICA approach to one generated using the same approach but with fine spatial resolution images for both time-1 and time-2. We found that the adoption of a backdating approach improves the efficiency of the analysis by focusing only on the change area, which typically represents a small part of urban and peri-urban areas. We also found that the proposed method produced a change map with an overall accuracy that is relatively large, and slightly larger than that of the change map produced with datasets of similar fine spatial resolution. However, some of the user's and producer's accuracy obtained in the study were small.

Future studies could refine and test procedures for more detailed classification schemes, such as to map socio-economic status of residential areas, by taking advantage of finer spatial and radiometric resolutions of satellites and aerial images that are becoming ubiquitous. Finally, researchers performing land cover land use change analysis without access to FRes data due either to lack of coverage or financial resources could benefit from the findings of this research.

Acknowledgements

This research was supported by the Interdisciplinary Research in Earth Science (IDS) program of the National Aeronautics and Space Administration (NASA), NASA award number G00009708. NASA and the National Geospatial-Intelligence Agency (NGA) provided fine spatial resolution, commercial satellite imagery through the NextView license agreement, with tremendous assistance from Jaime Nickeson of NASA Goddard Space Flight Center.

References

Belgiu, M., Drăguţ, L., Strobl, J., 2014. Quantitative evaluation of variations in rule-based classifications of land cover in urban neighbourhoods using WorldView-2 imagery. ISPRS J. Photogramm. Remote Sens. 87, 205–215.
Bouziani, M., Goita, K., He, D.C., 2010. Rule-based classification of a very high resolution image in an urban environment using multispectral segmentation guided by cartographic data. IEEE Trans. Geosci. Remote Sens. 48 (8), 3198–3211.
Chen, G., Hay, G.J., Carvalho, L.M., Wulder, M.A., 2012. Object-based change detection. Int. J. Remote Sens. 33 (14), 4434–4457.
Cochran, W.G., 1977. Sampling Techniques, third ed. John Wiley & Sons, New York.
Ghana Statistical Service, 2012. 2010 Population & Housing Census Summary Report of Final Results. Ghana Statistical Service, Accra.
Gupta, S., Mazumdar, S.G., 2013. Sobel edge detection algorithm. International Journal of Computer Science and Management Research 2 (2), 1578–1583.
Haklay, M., Weber, P., 2008. Openstreetmap: user-generated street maps. IEEE Pervasive Computing 7 (4), 12–18.
Hay, G.J., Castilla, G., 2008. Geographic object-based image analysis (GEOBIA): a new name for a new discipline. Object-Based Image Analysis 75–89.
Jensen, R., 2016. Introductory Digital Image Processing, A Remote Sensing Perspective, 4th Ed. Prentice-Hall, Inc., New Jersey.
Linke, J., McDermid, G.J., Pape, A.D., McLane, A.J., Laskin, D.N., Hall-Beyer, M., Franklin, S.E., 2009. The influence of patch-delineation mismatches on multi-temporal landscape pattern analysis. Landsc. Ecol. 24 (2), 157–170.
Ma, L.G., Deng, J.S., Yang, H., Hong, Y., Wang, K., 2015. Urban landscape classification using Chinese advanced high-resolution satellite imagery and an object-oriented multi-variable model. Frontiers of Information Technology & Electronic Engineering 16 (3), 238–248.
McFeeters, S.K., 1996. The use of the normalized difference water index (NDWI) in the delineation of open water features. Int. J. Remote Sens. 17 (7), 1425–1432.
Møller-Jensen, L., Kofie, R.Y., Yankson, P.W., 2005. Large-area urban growth observations—a hierarchical kernel approach based on image texture. Geografisk Tidsskrift-Danish Journal of Geography 105 (2), 39–47.
Momeni, R., Aplin, P., Boyd, D.S., 2016. Mapping complex urban land cover from spaceborne imagery: the influence of spatial resolution, spectral band set and classification approach. Remote Sens. 8 (2), 88.
Myint, S.W., Gober, P., Brazel, A., Grossman-Clarke, S., Weng, Q., 2011. Per-pixel vs. object-based classification of urban land cover extraction using high spatial resolution imagery. Remote Sens. Environ. 115 (5), 1145–1161.
Odindi, J., Mhangara, P., Kakembo, V., 2012. Remote sensing land-cover change in Port Elizabeth during South Africa's democratic transition. S. Afr. J. Sci. 108 (5–6), 60–66.
Olofsson, P., Foody, G.M., Herold, M., Stehman, S.V., Woodcock, C.E., Wulder, M.A., 2014. Good practices for estimating area and assessing accuracy of land change. Remote Sens. Environ. 148, 42–57.
Stow, D., 2009. Geographic object-based image change analysis. In: Fischer, Manfred, Geti, Arthur (Eds.), Handbook of Spatial Analysis. Springer, Berlin, pp. 565–582.
Stow, D.A., Weeks, J.R., Shih, H.C., Coulter, L.L., Johnson, H., Tsai, Y.H., Kerr, A., Benza, M., Mensah, F., 2016. Inter-regional pattern of urbanization in southern Ghana in the first decade of the new millennium. Appl. Geogr. 71, 32–43.

Toure, S., Stow, D., Shih, H.C., Coulter, L., Weeks, J., Engstrom, R., Sandborn, A., 2016. An object-based temporal inversion approach to urban land use change analysis. Remote Sensing Letters 7 (5), 503–512.
Wang, L., Li, C., Ying, Q., Cheng, X., Wang, X., Li, X., Hu, L., Liang, L., Yu, L., Huang, H., Gong, P., 2012. China's urban expansion from 1990 to 2010 determined with satellite remote sensing. Chin. Sci. Bull. 57 (22), 2802–2812.
Xian, G., Homer, C., Fry, J., 2009. Updating the 2001 National Land Cover Database land cover classification to 2006 by using Landsat imagery change detection methods. Remote Sens. Environ. 113 (6), 1133–1147.
Yu, W., Zhou, W., Qian, Y., Yan, J., 2016. A new approach for land cover classification and change analysis: integrating backdating and an object-based method. Remote Sens. Environ. 177, 37–47.
Zhou, W., Troy, A., Grove, M., 2008. Object-based land cover classification and change analysis in the Baltimore metropolitan area using multitemporal high resolution remote sensing data. Sensors 8 (3), 1613–1636.